Nigerian Journal of Physics (NJP)
ISSN online: 3027-0936
ISSN print: 1595-0611
DOI: https://doi.org/10.62292/njp.v35(s).2026.666
Volume 35(S), 2026

Geoelectric Characterization and Groundwater Potential Mapping of Nguru Local Government Area, Chad Basin, Northeastern Nigeria

*[1]Isa Muhammad Sani, [2]Olatunji Samuel Ayanninuola and [3]Obrike Stephen Ewoma

[1]Department of Physics, Yobe State University, Damaturu, Nigeria.
[2]Department of Physics, Nasarawa State University, Keffi, Nigeria.
[3]Department of Geology, Nasarawa State University, Keffi, Nigeria.

*Corresponding Author's Email: almasmuhammad009@gmail.com Phone: +2347033773882

Keywords:
X-Ray,
Simulation,
Radiation

Submitted: 23 July 2026

Accepted: 17 Aug. 2026

Published: 25 Aug. 2026

ABSTRACT

The geoelectric investigation was carried out in Nguru Local Government Area (LGA), Yobe State, within the Chad Basin of Northeastern Nigeria, to evaluate groundwater potential and delineate subsurface lithology. The study area is underlain predominantly by the Chad Formation, comprising unconsolidated to weakly consolidated sand, clay and sandy-clay deposits of fluvial and lacustrine origin. These alternating permeable and relatively low-permeability units form the principal aquifer–aquitard framework of the area. One hundred (100) Vertical Electrical Soundings (VES) were carried out using the Schlumberger electrode configuration with a maximum current-electrode half-spacing (AB/2) of 200 m. WinResist software was used for partial curve matching and one-dimensional forward modelling. The results revealed five to six geo-electric strata with resistivity values ranging from 0.5 to 1941.3 Ωm. Seventeen curve types were identified, with KHK (19%) and KQH (19%) being the most common. The lithological categories identified were topsoil, lateritic/hard clay, clay, sandy clay and sand. A major NW–SE-trending sand-rich buried channel-like feature was delineated, with maximum interpreted sand-bearing thickness of 88.7 m at Yamdugu (VES 86). The Groundwater Potential Index classified the area into HIGH (5%), MODERATE (70%) and LOW (25%) zones. Sixteen priority locations were identified for further borehole investigation. Validation data supplied from 25 borehole logs were compared with the VES interpretations; the existing scatter plot contains 10 numerical paired observations and gives $r = 0.993$ and $R^2 = 0.985$. The study provides a regional geoelectrical framework for groundwater exploration in Nguru LGA.

INTRODUCTION

In arid and semi-arid areas, where surface water is scarce and intermittent, groundwater is the most reliable water source (Todd & Mays, 2005). In the Sahel savanna area of Northeastern Nigeria, which includes Yobe State, the yearly precipitation is minimal (400-600 mm) and evapotranspiration levels are high, leading to surface water availability for only 4-5 months of the year (Obaje, 2009). The groundwater has become the primary source of water for domestic, agricultural and industrial purposes.

Nguru Local Government Area (LGA) in the Chad Basin of northern Yobe State is predominantly dependent on underground water sources. The community has more than 300,000 (NPC, 2006) people who get their water from shallow hand-dug wells and boreholes. A large number of boreholes drilled in the region have been unsuccessful or of low yield due to poor siting, as a result of inadequate geophysical evaluation. There is a critical gap in understanding of subsurface lithology, aquifer geometry and groundwater potential leading to arbitrary and unsustainable extraction of groundwater.

The Vertical Electrical Sounding (VES) technique is a proficient tool in groundwater investigation to distinguish subsurface strata according to their electrical resistivity differences (Telford et al., 1990). The technique is rapid, inexpensive and non-intrusive, making it suitable for regional groundwater research (Zohdy et al., 1974).

Earlier geophysical works in the Chad Basin have mapped the resistivity values of different lithologies and revealed the presence of multi-aquifer systems at Maiduguri (Adamu et al., 2018), Geidam (Lariski et al., 2021) and other parts of Yobe State (Mohammed et al., 2012). But before this study, no detailed VES investigation covering the entire Nguru LGA (916 km^2) with 100 stations had been conducted.

The study was undertaken to characterize the subsurface geo-electric strata and their resistivity parameters, relate the geo-electric units to lithological characteristics, delineate aquifer-bearing zones, assess the distribution of VES curve types and protective properties, delineate groundwater potential zones, and identify priority areas for further borehole development within Nguru LGA.

MATERIALS AND METHODS

Study Area

Location and Physiography

The research area is located in the Sahelian savanna climate, with a distinct wet season (June–September) and dry season (October–May). The terrain is largely flat, with reported elevations of about 330–350 m above sea level. Hydrogeologically, groundwater occurs mainly within sand-rich horizons of the Chad Formation, while clay and sandy-clay units act as aquitards or lower-permeability intervals.

Geological Setting

The study area is underlain predominantly by the Chad Formation (Upper Pliocene–Pleistocene), comprising continental sands, clays and sandy clays deposited under fluvial and lacustrine conditions (Barber, 1965). In Nguru, the formation is reported to attain substantial thickness and contains alternating permeable sand and less-permeable clay units that control groundwater occurrence and movement (Adamu et al., 2018). The shallow subsurface also contains locally developed lateritic/hard clay. The geological map of Nguru LGA was prepared from the Geological and Mineral Resouces Map of Yobe State published by the Nigeria Geological Survey Agency (2006), as in Figure 1.

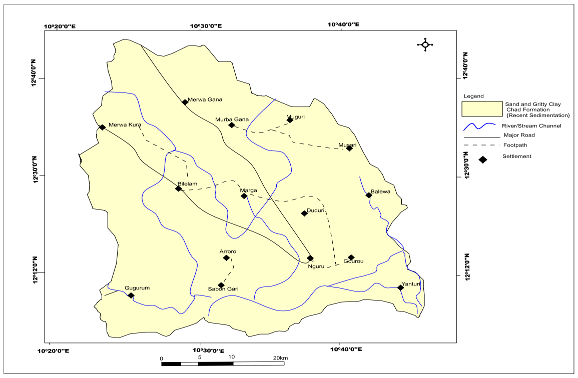

Figure 1: Geological Map of Nguru LGA Showing the Chad Formation (Adopted from NGSA, 2006)

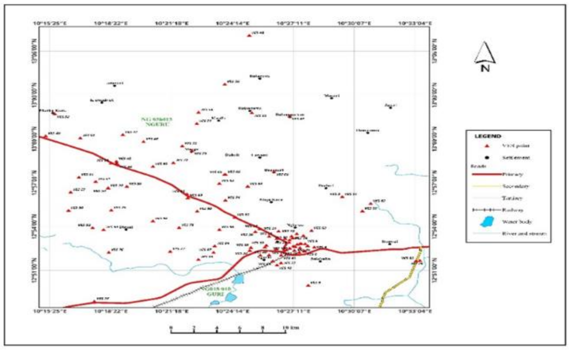

Figure 2: Location Map of Nguru LGA showing 100 VES Stations

Field Data Acquisition

A total of 100 VES measurements were acquired with a Herojat Terrameter using the Schlumberger electrode configuration. At each station, the two outer electrodes (A and B) were used to inject a controlled electrical current into the ground, while the two inner electrodes (M and N) measured the resulting potential difference (ΔV). The current-electrode separation was progressively increased to investigate greater depths, while the potential electrodes were maintained near the centre of the array and repositioned when necessary to maintain measurable potential differences. The measured current and potential difference, together with the Schlumberger geometric factor, were used to calculate apparent resistivity. A schematic of the electrode arrangement and current/potential measurement is presented in Figure 2.

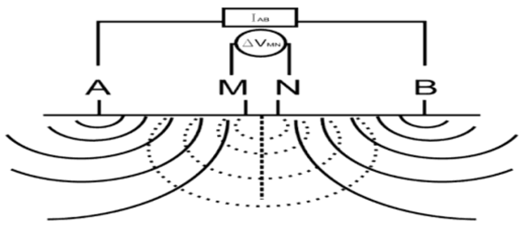

Figure 3: Schlumberger Electrode Configuration Showing Current Electrodes (A, B), Potential Electrodes (M, N), Current Flow Lines, and Equipotential Surfaces (U. S. Environmental Protection Agency, n.d.)

The spacing of the current electrodes (AB/2) was varied from 1 m to 200 m at each VES station. The apparent resistivity (ρa) was calculated from the measured current, potential difference and electrode geometry as follows:

$$\rho a = K \frac{\Delta V}{I} = K \times R \qquad (1)$$

Where

$$K = \pi \left(\frac{AB^2}{MN} - \frac{MN}{4} \right) \qquad (2)$$

$$R = \frac{\Delta V}{I} \qquad (3)$$

Where ΔV potentials at M and N, R is resistance of the ground, K is Geometric constant, AB is Current electrode separation and MN Potential electrode separation. Coordinates were recorded at each station using a Garmin GPS Map 62s.

Data Processing and Interpretation

The apparent resistivity measurements were plotted as a function of AB/2 on bi-logarithmic paper to obtain field curves. Initial analysis was carried out by partial curve matching with two-layer master curves and additional point charts (Orellana & Mooney, 1966). Preliminary models were refined using the WinResist software with an acceptable root mean square error of less than 10%.

Lithological Interpretation

The lithological interpretation was based on the ranges observed in the 100 VES models and their hydrogeological significance in the Chad Basin. To remove the inconsistency between Tables 1 and 2, the same resistivity boundaries used to summarize the interpreted lithologies in Table 2 are adopted consistently in the classification.

Table 1: Resistivity Range, Lithology, and Hydrogeological Significance

Resistivity Range (Ωm)	Lithology	Hydrogeological Significance
< 5.0	Clay	Aquitard
5.0–12.6	Clay / Sandy Clay	Aquitard to poor aquifer
12.7–39.8	Sandy Clay	Poor to moderate aquifer
40.0–100.0	Sand (fine to medium)	Moderate aquifer
100.1–304.5	Sand (coarse / relatively resistive)	Favourable aquifer
> 304.5	Lateritic/Hard Clay	Protective/non-aquifer where confirmed by lithology

Derivation of Aquifer Parameters

The total sand thickness (H_s) was obtained as the summation of all the layers having resistivity more than 40 Ωm. Depth to the aquifer (D_a) was taken as the depth to the first substantial sand layer (ρ >40 Ωm, thickness >5 m). The protective capacity was evaluated by measuring the total thickness of the clay and sandy clay layers above the main aquifer, using empirical methods (Olorunfemi & Fasuyi, 1993).

Validation

VES interpretations were validated using 25 borehole lithology logs distributed across 11 validation clusters obtained from the Rural Water Supply and Sanitation Agency (RUWASA), Yobe State.

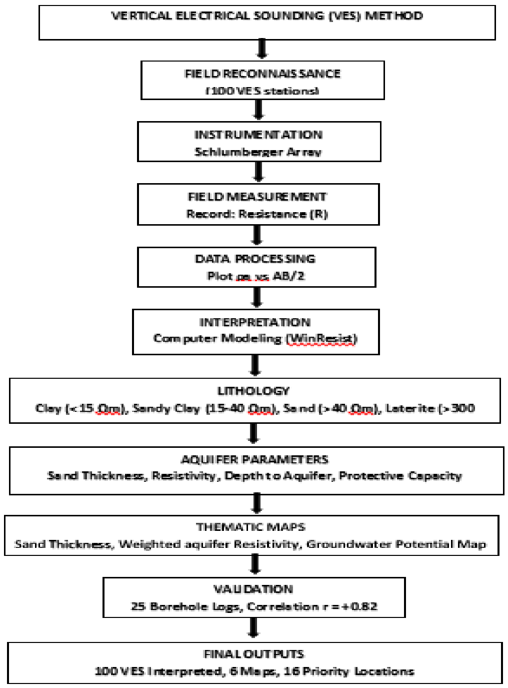

Figure 4: Procedure for Vertical Electrical Sounding Data Acquisition and Interpretation

RESULTS AND DISCUSSION

Geo-electric Layers and Resistivity Distribution

The 100 VES stations revealed five to six geo-electric layers, with resistivity values ranging from 0.5 Ωm to 1941.3 Ωm. Five main lithological categories were identified: Topsoil, Lateritic/Hard Clay, Clay, Sandy Clay and Sand. The resistivity intervals in Table 1 were used as interpretive guidelines for assigning lithological and hydrogeological significance to the VES layers. Because resistivity is influenced by lithology, moisture content, clay fraction, grain size and pore-water salinity, the observed resistivity values of the interpreted units are not expected to form mutually exclusive ranges. Table 2 therefore presents the ranges actually observed among the 100 VES models and should not be interpreted as independent classification thresholds. Lithological assignment was based on the Table 1 criteria together with layer thickness, curve characteristics and the geological setting of the Chad Formation. A summary of the observed geo-electric strata and lithological interpretation is presented in Table 2.

Table 2: Observed Resistivity and Thickness Ranges of Interpreted Geo-Electric Units

Lithology	Resistivity Range (Ωm)	Thickness Range (m)
Topsoil	3.7 - 1347.3	0.3 - 6.4
Lateritic/Hard Clay	84.1 - 1941.3	1.2 - 31.1
Clay	0.5 - 12.6	2.4 - 79.4
Sandy Clay	10.1 - 39.8	5.1 - 72.8
Sand	40.0 - 304.5	5.0 - 83.2

The VES stations were distributed across the study area using a grid pattern with an average spacing of approximately 3 km in rural areas (villages) and in the urban area (Nguru main town) random selection where carried out to ensure regional coverage to cover the whole wards. This spacing was chosen to capture the lateral variations in lithology and aquifer geometry while maintaining practical field logistics. Aquifer units were interpreted based on the following criteria: resistivity values >40 Ωm, layer thickness >5 m to ensure significant aquifer potential, and presence of protective clay layers above the aquifer to ensure water quality protection.

Curve Types

Seventeen different types of curves were found (Table 3). The most common were KHK (19%) and KQH (19%). The KHK configuration ($\rho_1 < \rho_2 > \rho_3 < \rho_4 > \rho_5$) exhibits a sequence of resistive topsoil, conductive clay, resistive sand, and conductive clay, which is most advantageous for groundwater occurrence because it situates the aquifer between protective clay layers. The KQH configuration ($\rho_1 < \rho_2 > \rho_3 > \rho_4 < \rho_5$) indicates a more complex pattern with multiple conductive layers, suggesting the presence of intervening clay and sandy clay layers with occasional sand lenses.

Table 3: Distribution of VES Curve Types

Curve type	Curve Characteristics	Frequency	Curve type (%)
AKH	ρ1<ρ2<ρ3>ρ4<ρ5	1	1
AKQ	ρ1<ρ2<ρ3>ρ4>ρ5	1	1
HAA	ρ1>ρ2<ρ3<ρ4<ρ5	2	2
HAK	ρ1>ρ2<ρ3<ρ4>ρ5	3	3
HKH	ρ1>ρ2<ρ3>ρ4<ρ5	11	11
HKQ	ρ1>ρ2<ρ3>ρ4>ρ5	2	2
KHA	ρ1<ρ2>ρ3 <ρ4<ρ5	11	11
KHAK	ρ1<ρ2>ρ3 <ρ4<ρ5> ρ6	1	1
KHK	ρ1<ρ2>ρ3 <ρ4>ρ5	19	19
KHKQ	ρ1<ρ2>ρ3 <ρ4>ρ5> ρ6	1	1
KQH	ρ1<ρ2>ρ3 >ρ4<ρ5	19	19
KQQ	ρ1<ρ2>ρ3 >ρ4>ρ5	12	12
QHA	ρ1>ρ2>ρ3<ρ4<ρ5	3	3
QHK	ρ1>ρ2>ρ3<ρ4>ρ5	6	6
QQH	ρ1>ρ2>ρ3>ρ4<ρ5	6	6
QQHK	ρ1>ρ2>ρ3>ρ4<ρ5> ρ6	1	1
QQQH	ρ1>ρ2>ρ3>ρ4>ρ5< ρ6	1	1
Total		100	100

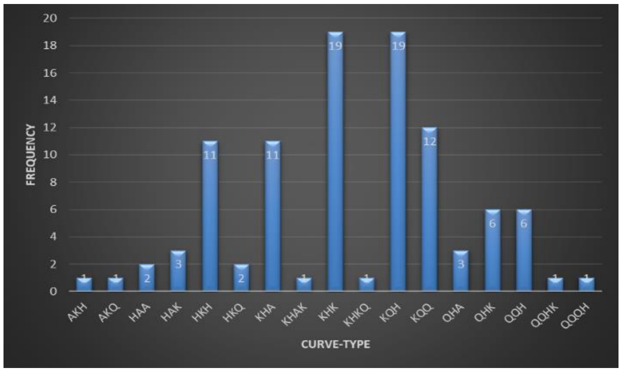

Figure 5: Frequency Distribution of Curve Type of the Study Area

Lateritic Hardpan

A distinct high-resistivity (84.1–1941.3 Ωm) layer identified as lateritic hardpan is extensively distributed. Notable examples include VES 96 (1941.3 Ωm), VES 32 (1910.7 Ωm), VES 50 (1517.6 Ωm), and VES 62 (1502.3 Ωm). This layer offers excellent natural protection to the underlying aquifers but can be difficult to drill through mechanically.

Aquifer Characteristics and Paleo-Channel Discovery

Figure 6 presents the total sand thickness map showing a major NW-SE trending paleo-channel system extending from Baganari through Afunori to Yamdugu and Dumsai. Total sand thickness ranges from 0 to 88.7 m, with the thickest accumulations at Yamdugu (88.7 m), Dumsai (84.6 m), and Gamu (83.2 m). Weighted aquifer resistivity ranges from 11.4 to 304.5 Ωm.

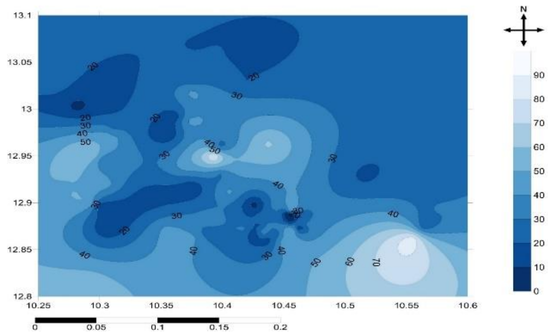

Figure 6: Total Sand Thickness Map of Study Area Showing the NW-SE Trending Paleo-Channel

Weighted Aquifer Resistivity

The weighted aquifer resistivity map (Figure 7) presents the spatial distribution of average resistivity of sand layers weighted by their thickness, representing the quality of aquifer materials across Nguru LGA. Higher values (>100 Ωm) indicate coarse, clean sands with excellent permeability, while lower values (<40 Ωm) indicate fine sands or sandy clay with reduced permeability.

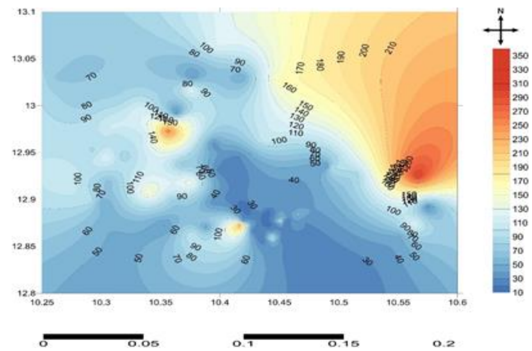

Figure 7: Weighted Aquifer Resistivity Map of Study Area

Groundwater Potential Zonation

Three groundwater-potential zones were delineated by integrating total sand-bearing thickness and weighted aquifer resistivity into a normalized Groundwater Potential Index (GWPI). The final area proportions are reported consistently as HIGH (5%), MODERATE (70%) and LOW (25%). The spatial distribution of these zones is presented in Figure 8.

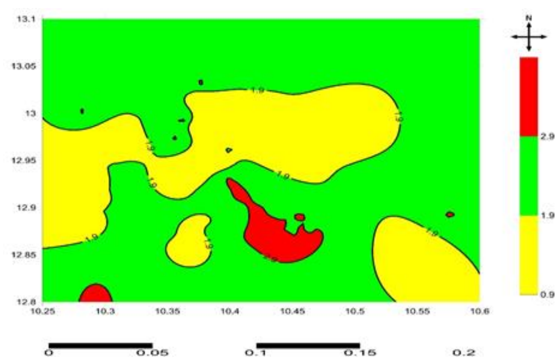

Figure 8: Groundwater Potential Zonation Map of the Study Area

LOW Potential Zone (Yellow / Index < 1.9): Covers 25% of the area. Characterized by thin sand packages (<15 m) or highly conductive clay matrices (ρ < 40 Ωm), yielding expected borehole discharge of less than 2 L/s.

MODERATE Potential Zone (Green / Index 1.9-2.9): Forms the dominant regional hydrogeological framework, covering 70% of Nguru LGA. Sand thicknesses range from 15-30 m with intermediate resistivities (40-80 Ωm), providing sustainable domestic yields between 2 and 5 L/s.

HIGH Potential Zone (Index > 2.9): This zone covers approximately 5% of the study area and occurs mainly in localized segments of the interpreted sand-rich buried channel-like feature and other areas where relatively thick sand-bearing sequences coincide with favourable resistivity. Sand thickness exceeds 30 m with optimal coarse sand resistivities (>80 Ωm), capable of high-yield commercial development (>5 L/s). These locations are considered priority targets for further borehole investigation, subject to confirmation by drilling and pumping tests.

Table 4: Groundwater Potential Zones Summary

Zone	Map Contour index	Sand Thickness (m)	Resistivity (Ωm)	Area (%)	Expected Yield (L/s)
HIGH (Dark Red)	2.9	30	80	5	5
MODERATE (Green)	1.9-2.9	15-30	40-80	70	2-5
LOW (Yellow)	<1.9	<15	<40	25	<2

Priority Locations

Sixteen priority locations were identified for high-yield borehole development. The top five locations are: Baganari (VES 68: 62.5 m sand, 106.1 Ωm), Yamdugu (VES 86: 88.7 m sand, 58.0 Ωm), Dumsai (VES 85: 84.6 m sand, 48.3 Ωm), Sinidi (VES 51: 60.1 m sand, 86.6 Ωm), and Gamu (VES 54: 83.2 m sand, 48.1 Ωm).

Table 5: Correlation Between VES Data and Borehole Log

Validation pair	VES-derived sand-bearing thickness (m)	Borehole-confirmed aquifer thickness (m)
1	84.6	56.6
2	42.9	26.0
3	31.4	23.4
4	28.7	18.1
5	26.9	16.2
6	32.2	22.2
7	32.9	22.1
8	16.9	12.1
9	12.6	11.6
10	5.1	3.4

Validation with Borehole Logs

To validate the VES interpretations, 25 borehole lithology logs from 10 validation clusters were compared with VES-derived lithological sequences. Figure 10 presents a side-by-side correlation of VES and borehole logs for selected validation points.

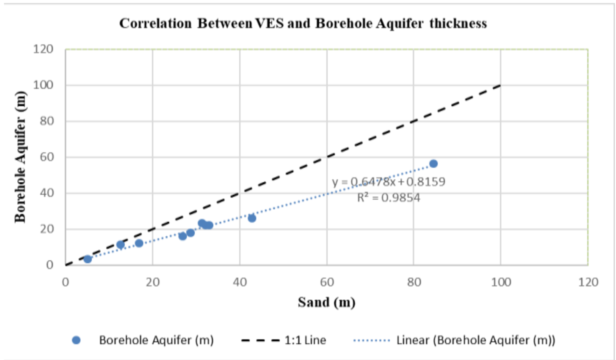

Figure 9: Scatter Plot Showing the Relationship Between VES-Derived Total Sand Thickness and Borehole-Confirmed Aquifer Thickness for the 10 Numerical Validation Observations (n = 10)

Validation matching at 10 key structural locations with 25 composite borehole logs revealed a strong positive correlation (r = +0.993, R^2 = 0.985) between VES-derived total sand thickness and actual borehole-confirmed aquifer thickness (Figure 6). The linear relationship is mathematically described by:

$$y = 0.6478x + 0.8159 \quad (4)$$

This indicates that the actual productive sand-aquifer thickness accounts for approximately 65% of the overall VES-interpreted sand thickness sequence due to minor structural clay intersections.

The correlation coefficient (r = +0.993) confirms the reliability of VES results in predicting aquifer thickness across the study area.

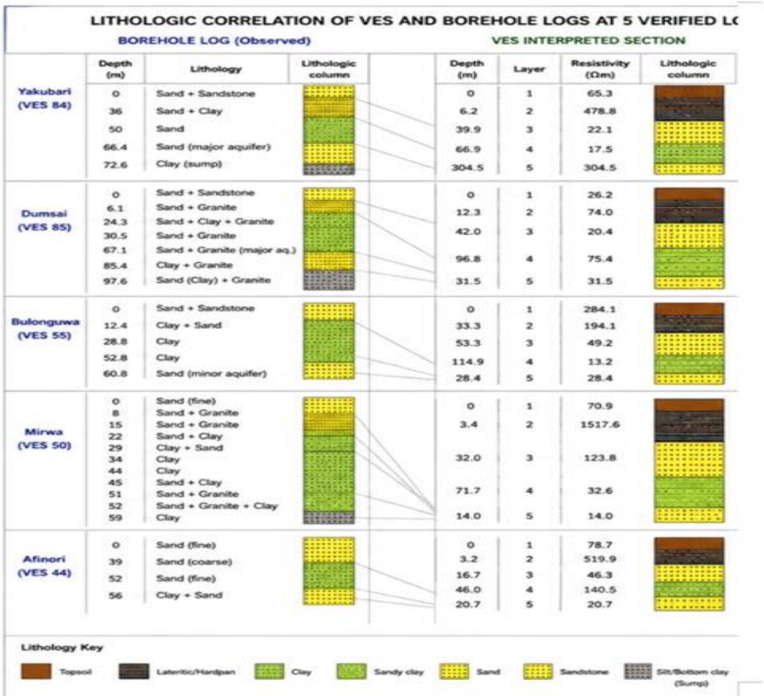

Figure 9: Side-by-side Correlation of Borehole Logs and VES VES Interpreted Lithology at Five Verified Locations

The regression slope indicates that the borehole-confirmed aquifer thickness is, on average, lower than the broader VES-derived sand-bearing thickness. This difference is consistent with the fact that VES interpretation may include mixed sand–clay intervals that are not counted as fully productive aquifer material in borehole lithological logs.

CONCLUSION

This geoelectric investigation of 100 VES stations across Nguru LGA has successfully characterized the subsurface lithology and groundwater potential of the area. The following conclusions are drawn:

i. The sub-surface is made up of 4-6 geo-electric strata that correspond to 5 major lithological units, confirming the complex alluvial sand/clay sequence of the Chad Formation.
ii. Seventeen different curve types were identified, with KHK (19%) and KQH (19%) being predominant.
iii. A major NW-SE trending paleo-channel system was discovered with a maximum sand thickness of 88.7 m at Yamdugu (VES 86).
iv. Index contours were used to delineate three groundwater potential areas namely HIGH (5%), MODERATE (70%) and LOW (25%) indicating the dominance of aquifers of moderate yield in the region.
v. Sixteen priority locations were identified for high-yield borehole development, with Baganari (VES 68), Yamdugu (VES 86), and Dumsai (VES 85) ranking highest.
vi. Empirical validation using 25 borehole logs confirmed a strong correlation coefficient (r = +0.993) and also validating the reliability of VES results for groundwater exploration in the Chad Basin.

ACKNOWLEDGEMENT

The authors are grateful to the traditional leaders and community members of Nguru LGA for their cooperation during fieldwork. Special thanks to the Rural Water Supply and Sanitation Agency (RUWASA), Yobe State, for providing the critical borehole calibration logs. The Department of Physics, Yobe State University, is acknowledged for providing the necessary geophysical instruments.

CONFLICT OF INTEREST

The authors declare that there is no conflict of interest regarding the publication of this paper.

SOURCES OF FUNDING

This research received no specific grant from any funding agency in the public, commercial, or not-for-profit sectors.

REFERENCES

Agada, L. E. (2021). Geophysical and hydrochemical investigation of the impact of flood on groundwater in Nguru, Nigeria. FUDMA Journal of Sciences, 5(4), 426–431. https://doi.org/10.33003/fjs-2021-0504-2061

Barber, W. (1965). Pressure water in the Chad Formation of Bornu and Dikwa Emirates, northeastern Nigeria. *Geological Survey of Nigeria Bulletin*, 35, 1-138.

Mohammed, M. Z., Olorunfemi, M. O., & Idonigie, A. I. (2012). Geoelectric sounding for evaluating soil corrosivity and the vulnerability of porous media aquifers in parts of the Chad Basin Fadama floodplain, northeastern Nigeria. Journal of Sustainable Development, 5(7), 111–126. https://doi.org/10.5539/jsd.v5n7p111

Adamu, S., Bukar, M., & Sadiq, H. M. (2018). Hydrogeological windows in the upper aquifer of the Chad Formation in the Chad Basin, North-Eastern Nigeria. International Journal of Research - GRANTHAALAYAH, 6(3), 30–38. https://doi.org/10.29121/granthaalayah.v6.i3.2018.1495

NPC (National Population Commission). (2006). 2006 Population and Housing Census. Abuja, Nigeria.

Obaje, N. G. (2009). Geology and mineral resources of Nigeria. *Springer-Verlag*.

Olorunfemi, M. O., & Fasuyi, S. A. (1993). Aquifer types and the geoelectric/hydrogeologic characteristics of part of the central basement terrain of Nigeria (Niger State). Journal of African Earth Sciences, 16(3), 309–317. https://doi.org/10.1016/0899-5362(93)90051-Q

Orellana, E., & Mooney, H. M. (1966). Master tables and curves for vertical electrical sounding over layered structures. I*nterciencia*.

Lariski, F. M., Geidam, I. G., & Madaki, U. Y. (2021). Application of electrical resistivity method (ERM) and aeromagnetic methods in mapping ground water potentials: A case study of Fune and Nangere areas of Yobe State, Nigeria. Global Scientific Journal, 9(9), 2251–2265. https://www.globalscientificjournal.com/researchpaper/Application_of_Electrical_Resistivity_ERM_and_Aeromagnetic_Methods_in_Mapping_Underground_Water_Potentials_A_Case_Study_of_Nangere_and_Fune_L_G_Area_of_Yobe_State_Nigeria_.pdf

Nigeria Geological Survey Agency (2006). Geological and Mineral Resouces Map of Yobe State, Nigeria (Scale 1;400,000)[Geological Map]. Abuja, Nigeria: Nigeria Geological Survey Agency

Geological Map of Yobe State, 1: 400Telford, W. M., Geldart, L. P., & Sheriff, R. E. (1990). *Applied geophysics (2nd ed.)*. Cambridge University Press.

Todd, D. K., & Mays, L. W. (2005). *Groundwater hydrology (3rd ed.)*. John Wiley and Sons.

U.S. Environmental Protection Agency. (n.d.). Resistivity methods. CLU-IN. https://cluin.org/characterization/technologies/geophysics/pages/reference/methods/Surface_Geophysical_Methods/Electrical_Methods/Resistivity_Methods.htm

Zohdy, A. A. R., Eaton, G. P., & Mabey, D. R. (1974). Application of surface geophysics to groundwater investigations. U.S. *Geological Survey Techniques of Water-Resources Investigations*, Book 2, Chapter D1